J Therm Anal Calorim (2010) 99:563–570
DOI 10.1007/s10973-009-0159-4

Crystallization and melting behaviors of maleic anhydride grafted poly(propylene) nucleated by an aryl amide derivative

Bo Song · Yong Wang · Hongwei Bai · Li Liu · Yanli Li · Jihong Zhang · Zuowan Zhou

Received: 20 February 2009 / Accepted: 3 April 2009 / Published online: 19 June 2009

Abstract This paper reports the crystallization behavior of maleic anhydride grafted poly(propylene) (PP-MA) with an aryl amide derivative (TMB-5) as β-phase nucleating agent (β-NA). The isothermal and nonisothermal crystallization behaviors of PP-MA and nucleated PP-MA are comparatively researched based on the concentration of β-NA of 0.2 wt%. Subsequent melting behaviors after isothermal and nonisothermal crystallization process are also investigated to explore the crystalline structures formed during the crystallization. The results indicate that TMB-5 is an efficient β-NA in influencing the crystallization of PP-MA through increasing the crystallization rate and decreasing the fold surface free energy, leading to large amounts of β-phase formation during the crystallization process.

Keywords Aryl amide derivative · Isothermal and nonisothermal crystallization · Melting · PP-MA

Introduction

Isotactic poly(propylene) (iPP) is well known for its three common crystal forms, α, β and γ modification [1]. Among these crystal forms, β-PP has received considerable interests due to its excellent thermal and mechanical performance, especially high impact strength at low temperature [2, 3]. However, β-PP is in a metastable phase, it can be rarely obtained in a significant amount in commercial iPP products, unless crystallization conditions facilitating to the β-phase growth are taken [4, 5], such as quenching the melt to a certain temperature range [6], directional crystallization in a thermal gradient field [4, 5], shearing or elongation of the melt during crystallization process [7–10], vibration-induced crystallization [11], or using β-nucleating agent (β-NA) [2]. Of these methods, the addition of β-NA is the most effective to obtain a high level of the β-phase. The role of β-NA in inducing PP crystallization has been intensively researched. It has been widely accepted by researchers that the crystallization of PP nucleated by a NA includes two steps: one is the epitaxial growth of PP chain on the surface of the NA and the other is the growth of PP spherulites [12]. A certain epitaxial relationship between PP and the nucleating agent controls and accelerates heterogeneous nucleation and, finally determines the nucleation efficiency of such NA.

In the present work, maleic anhydride grafted poly (propylene) (PP-MA) was used and it is of considerable industrial interest to enhance its compatibility, adhesion and reactivity [13]. Aryl amides derivative (TMB-5) was used as β-NA for PP-MA. In the previous work, TMB-5 has been proved to be an efficient NA for iPP [14]. Here, we attempted to research the nucleation effect of TMB-5 on crystallization of PP-MA. The β-crystallization tendency of PP-MA has been reported recently [15]. Isothermal and nonisothermal crystallization behaviors and subsequent melting behaviors of nucleated PP-MA and neat PP-MA were comparatively researched through differential scanning calorimetry (DSC), polarized light microscope (PLM) and wide angle X-ray diffraction (WAXD) in this work.

B. Song · Y. Wang (✉) · H. Bai · L. Liu · Y. Li · J. Zhang · Z. Zhou
Key Laboratory of Advanced Technologies of Materials (Ministry of Education), School of Materials Science & Engineering, Southwest Jiaotong University, Chengdu 610031, China
e-mail: yongwang1976@163.com

Experimental

Materials

PP-MA (melt flow rate (MFR) of 29 g/10 min, 230 °C/2.16 kg) was obtained from Chengguang Institute of Chemical Engineering, China. MA group was randomly grafted onto the PP backbone, and the MA content in PP is 0.6 wt%. The β-phase NA aryl amides derivative (trademark: TMB-5) was supplied by Fine Chemicals Department of Shanxi Provincial Institute of Chemical Industry, China. Although we can not know the detailed chemical structure of this NA, it has been reported that TMB-5 has the similar chemical structure compared with some aromatic amine β-phase NA, such as *N*,*N*′-dicyclohexyl-2,6-naphthalenedicarboxamide, as shown in Scheme 1.

Sample preparation

Both PP-MA and NA were dried in an oven at 80 °C for 2 h prior to melt blending to eliminate the effect of moisture. A certain composition of PP-MA with 0.2 wt% NA (Shown as PP-MA/NA) was melt blended through using a Lab-station Brabender torque rheometer (Plasti-Corder, Germany) with the setting temperature of 185 °C. The melt blending time was 10 min and the rotor speed was 60 rpm. To provide same thermal history for both PP-MA and its nucleated sample, neat PP-MA was treated using exactly the same procedure as above. After that, the melt was cooled in the air.

Characterization

A Pyris-1 of Perkin-Elmer DSC was used for calorimetric investigation of the isothermal/non-isothermal crystallization and subsequent melting behaviors of samples. For isothermal crystallization process, about 5.0 mg sample was heated to 200 °C to erase the thermal history. After that, the sample was cooled down to a predetermined crystallization temperature at a cooling rate of 100 °C/min and crystallized at this temperature until the crystallization was finished completely. Subsequently, the sample was heated again to 200 °C at a heating rate of 10 °C/min. For nonisothermal crystallization process, once the sample was annealed at 200 °C, the sample was cooled down to room temperature at different cooling rates (5, 10, 20 and 40 °C/min). Subsequently, the sample was heated again to 200 °C. All the measurements were carried out in nitrogen atmosphere.

A Wide angle X-ray diffraction (WAXD, Panalytical X'pert PRO diffractometer with Ni-filtered Cu Kα radiation) was used to characterize the crystal structure of PP-MA and nucleated PP-MA obtained after being isothermal crystallized at 135 °C. The continuous scanning angle range was from 5° to 35° at 40 kV and 40 mA. The β-phase fraction (K_β) in the sample was calculated from WAXD diffractograms according to the following relation [16]:

$$K_\beta = I_{300}^{\beta}/(I_{110}^{\alpha} + I_{040}^{\alpha} + I_{130}^{\alpha} + I_{300}^{\beta}) \quad (1)$$

where I_{110}^{α}, I_{040}^{α} and I_{130}^{α} are the integral intensities of the (110), (040) and (130) reflections of α-phase, respectively, appearing at 2θ around 14.1, 16.9, 18.4°, respectively, and I_{300}^{β} is the integral intensity of (300) reflection of β-phase at 2θ around 16.1°.

The crystallization morphology of sample obtained through isothermal crystallization at 135 °C was characterized by a polarized light microscopy (XPN-203, China).

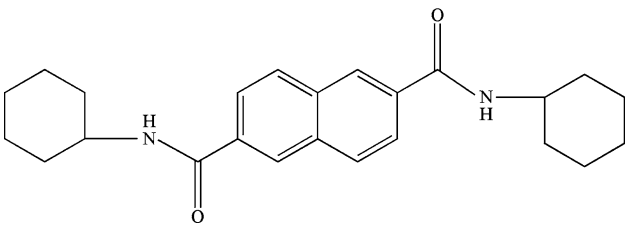

Scheme 1 Chemical structure of *N*,*N*′-dicyclohexyl-2,6-naphthalenedicarboxamide

Results and discussion

Isothermal crystallization and subsequent melting behaviors

Figure 1 shows the DSC heating curves of neat PP-MA and PP-MA/NA after isothermal crystallization at different temperatures as indicated. It can be observed that the peak temperature shifts to high temperatures with the increase of crystallization temperature (T_c), indicating thicker lamellae formation at relative higher T_c. For neat PP-MA, one can see that when T_c is below 130 °C, only a single melting peak is observed, otherwise, double melting peaks with a weak shoulder peak location at lower temperature are observed, indicating the formation of some lamellae with defect or smaller thickness at higher T_c, possibly due to the second crystallization in the interface of spherulites. PP-MA/NA sample presents double melting peaks at about 152.5–157 °C and 165 °C at low T_c. The left melting peak is ascribed to the fusion of β-phase, and the right one to α-phase (Shown as β and α_1, respectively) [17]. It also can be seen that the relative amount of β-phase gradually decreases with the increase of T_c applied in the work, and when crystallization temperature is at 142 °C, β-phase content is very small. This is due to the temperature is

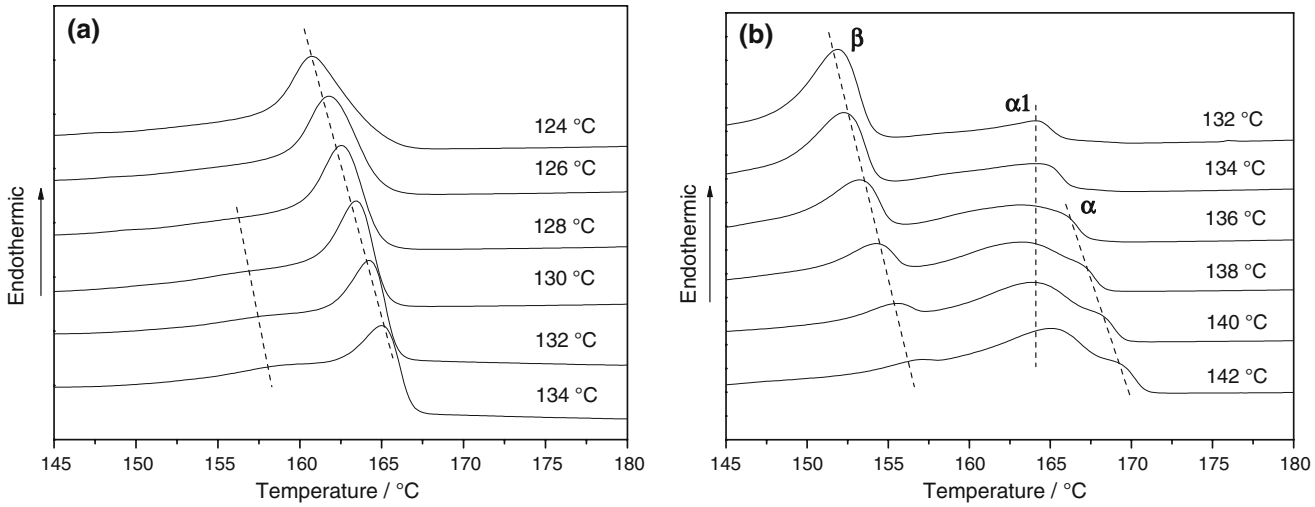

Fig. 1 DSC heating curves of **a** PP-MA and **b** PP-MA/NA samples after isothermal crystallization at the indicated temperatures

higher than the appropriate temperature for the β-phase growth (100–140 °C) [18]. When T_c is higher than 136 °C, a weak melting peak (α_2) at about 167–169 °C appears besides α_1, this shoulder peak gets stronger and shifts to high temperatures with the increase of T_c, possibly due to the fusion of reorganized α-phase from the melting of β-phase and poor perfect α-phase during the heating process [19].

To further prove the nucleation effect of TMB-5 on crystallization of PP-MA, isothermal crystallized neat PP-MA and PP-MA/NA samples were comparatively investigated through using WAXD and PLM, respectively, and the results are shown in Figs. 2 and 3. From Fig. 2 one can see that neat PP-MA crystallizes mainly in α-phase and PP-MA/NA mainly in β-phase. The relative content of β-phase was calculated as 75% according to the method

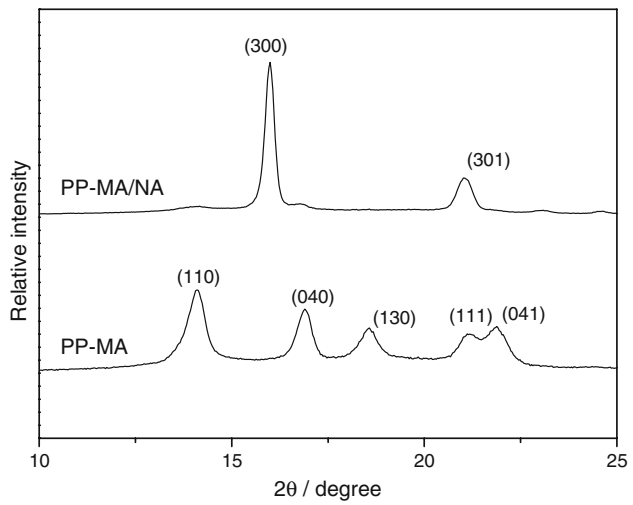

Fig. 2 WAXD profiles of PP-MA and PP-MA/NA. Samples were obtained after isothermal crystallization at 135 °C

proposed by Turner-Jones A [16], indicating that TMB-5 is very efficient as a β-phase NA in inducing PP-MA crystallization. This also can be proved by the crystallization morphology obtained during the isothermal crystallization. As shown in Fig. 3, neat PP-MA exhibits spherulites with diameters of about 100–200 μm, whereas much more homogeneous spherulites with diameters of about 5–10 μm are observed for PP-MA/NA sample, which means that the presence of TMB-5 increases the nucleation density of PP-MA greatly during the crystallization process.

Figure 4 shows the heat flow evolutions of virgin PP-MA and PP-MA/NA versus crystallization time. Although the T_c is different for virgin PP-MA and PP-MA/NA, one can notice that, once NA is introduced into PP-MA, the crystallization rate is enhanced greatly, shorter induction period of crystallization and narrower crystallization peaks are obtained in PP-MA/NA sample compared with neat PP-MA.

The isothermal crystallization of polymers can usually be well described by the Avrami equation [20]:

$$1 - X_t = \exp(-Kt^n) \tag{2}$$

where X_t is the relative degree of crystallinity at time t, n is the "Avrami exponent" which depends on the type of nucleation and the growth mechanism during the crystallization, K is a rate constant related to nucleation and growth rate parameters, and t is the time elapsed from the start of phase transformation. According to the Avrami equation, one formula can be got as follows:

$$\lg[-\ln(1 - X_t)] = n \lg t + \lg K \tag{3}$$

And generally, the plot of lg $[-\ln(1 - X_t)]$ versus lg t is a straight line. The slope of the line is n and the intercept with the ordinate yields lg K. From Eq. 3 the crystallization half time $t_{1/2}$ can be obtained by

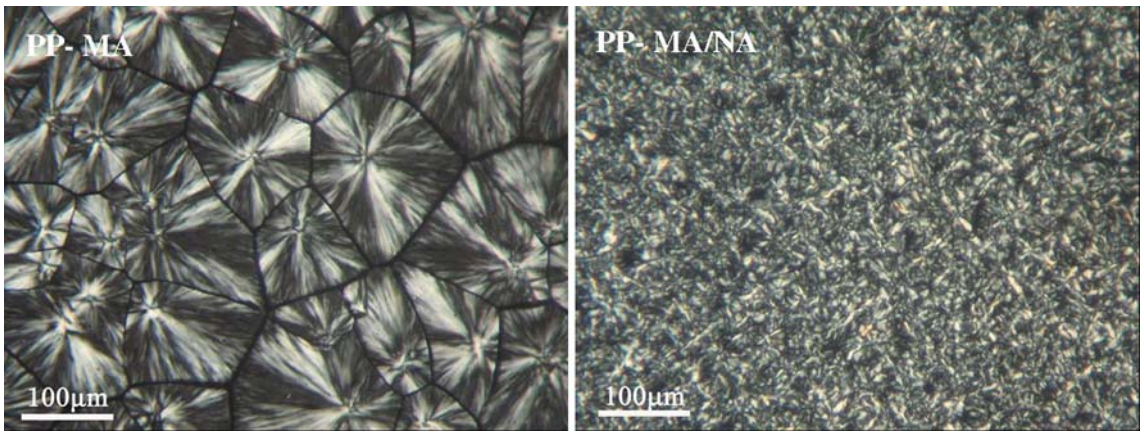

Fig. 3 PLM images of isothermal crystallization morphologies of PP-MA and PP-MA/NA

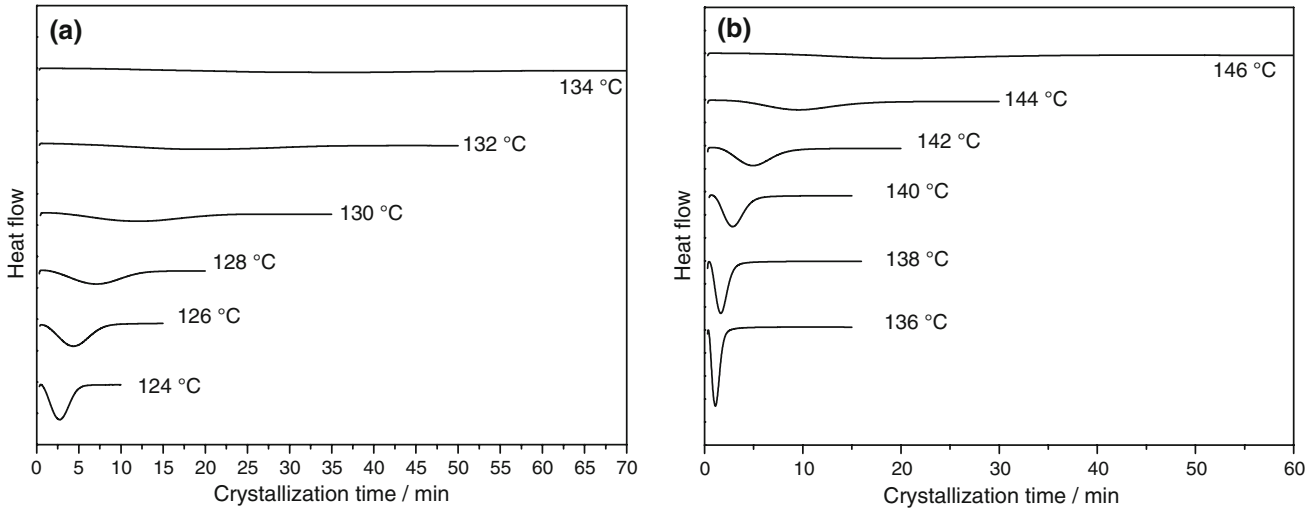

Fig. 4 DSC heat flow curves of **a** PP-MA and **b** PP-MA/NA samples during the isothermal crystallization process

$$t_{1/2} = (\ln 2/k)^{1/n} \tag{4}$$

Figure 5 shows the plots of lg $[-\ln(1 - X_t)]$ versus lg t, and the corresponding isothermal crystallization kinetics parameters are shown in Table 1. It is evident that, whether for neat PP-MA or for PP-MA/NA, the plots exhibit straight lines in the whole crystallization, which indicates that Avrami equation can satisfactorily describe the isothermal crystallization of PP-MA and PP-MA/NA and suggests that the crystallization of such samples is an one-step process. As shown in Table 1, PP-MA/NA sample has much smaller $t_{1/2}$ than PP-MA, suggesting the faster crystallization process. Furthermore, both PP-MA and PP-MA/NA exhibit the Avrami exponent values n of about 2–3, indicating that spherulite development arises from an athermal heterogeneous nucleation [21]. For neat PP-MA, it can be ascribed to a heterogeneous nucleation followed by diffusion-controlled spherulite growth due to the existence of impurities and catalyst residues during the chemical modification of PP.

The kinetic data of polymer isothermal crystallization can be analyzed using the spherulitic growth rate of the Hoffman-Lauritzen secondary nucleation theory, especially at melt-crystallization condition [22, 23].

$$G = G_o \exp\left[\frac{-U^*}{R(T_c - T_\infty)}\right] \exp\left[\frac{-K_g}{T_c \cdot \Delta T \cdot f}\right] \tag{5}$$

$$\ln G + \frac{U^*}{R(T_c - T_\infty)} = \ln G_o - \frac{K_g}{T_c \cdot \Delta T \cdot f} \tag{6}$$

where G_o is a constant of pre-exponential factor independent of temperature; U^* is the parameters describing the activation energy characteristic of the transport of the crystallizing segments across the liquid–crystal interface, universally $U^* = 6{,}280$ J/mol; R is the gas constant; T_∞ is the theoretical temperature at which all motions associated

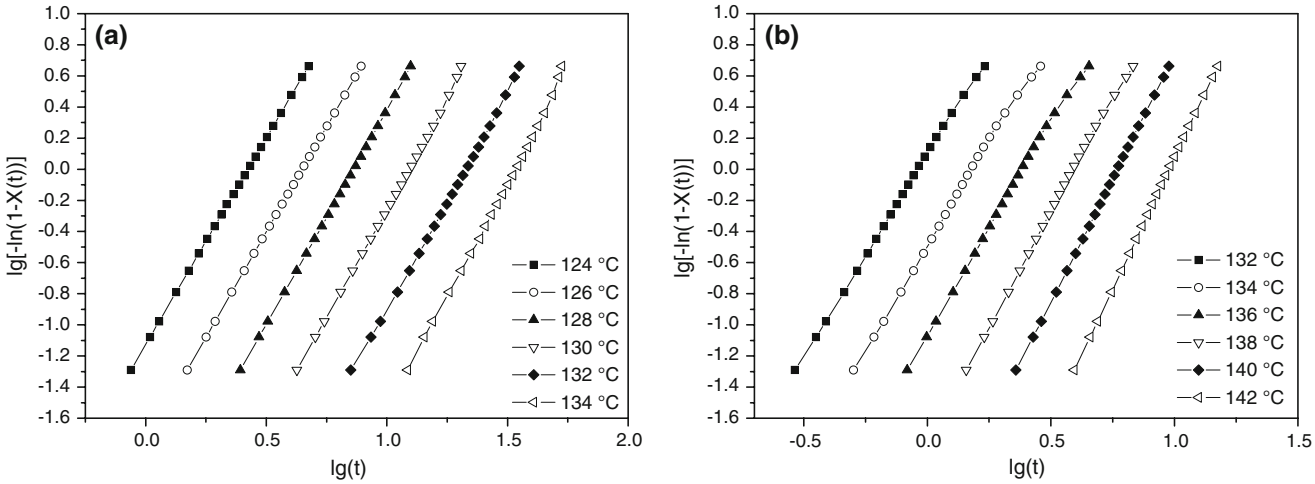

Fig. 5 Avrami plots of lg $[-\ln(1 - X_t)]$ vs. lg t for **a** PP-MA and **b** PP-MA/NA

Table 1 Isothermal crystallization kinetic parameters of neat PP-MA and PP-MA/NA

	PP-MA						PP-MA/NA					
T_c (°C)	124	126	128	130	132	134	132	134	136	138	140	142
n	2.66	2.71	2.74	2.76	2.78	2.85	2.53	2.63	2.71	2.94	3.08	3.33
$\overline{n}$	2.75						2.87					
lg k	−1.33	−1.76	−2.37	−3.02	−3.69	−4.38	0.06	−0.51	−1.07	−1.75	−2.40	−3.28
$t_{1/2}$ (min)	2.31	3.89	6.39	10.90	18.65	30.14	0.82	1.36	2.17	3.49	5.32	8.60
T_m^M (°C)	160.7	161.9	162.5	163.5	164.3	165.0	152.3	153.2	154.3	155.5	157.2	158.6
T_m^o (°C)	188.6						173.4					
σ_e (mJ/m^2)	98.14						35.61					
σ (mJ/m^2)	11.49						10.48					
K_g (10^5 K^2)	4.81						1.50					
L_m (nm)	16.54	17.27	17.70	18.40	19.03	19.57	8.52	8.89	9.42	10.05	11.09	15.15

with the viscous flow ceases and is defined as $T_\infty = T_g - C$, here C is a constant and in this paper $C \approx 30$ K; ΔT denotes the undercooling ($\Delta T = T_m^o - T_c$), here T_m^o is an equilibrium melting temperature; f is a corrective factor responsible for the variation of the equilibrium melting enthalpy with temperature, defined as $f = 2T_c/(T_m^o + T_c)$; and K_g is a nucleation constant as defined as:

$$K_g = 4b_o\sigma\sigma_e T_m^o/\Delta h_f k \tag{7}$$

where b_o is the monolayer thickness, σ is the lateral surface free energy, σ_e is the fold surface free energy, k is the Boltzmann constant ($k = 1.38 \times 10^{-23}$ J/K), and Δh_f is the enthalpy of fusion.

Equations 5–7 are applied for crystallization occurring in regimes I and III. From Eq. 6, the slop of plot of $\ln G + U^*/R(T_c - T_\infty)$ versus $1/T_c \cdot \Delta T \cdot f$ is K_g. From Eq. 7, K_g can be used to calculate the fold surface free energy σ_e. The plots of $\ln G + U^*/R(T_c - T_\infty)$ versus $1/T_c \cdot \Delta T \cdot f$ for neat PP-MA and PP-MA/NA and corresponding K_g values are shown in Fig. 6 and Table 1, respectively. Prior to determining σ_e, σ is estimated through using the following equation:

$$\sigma = \alpha(a_o b_o)^{1/2}\Delta h_f \tag{8}$$

where α is assumed empirically to be 0.1; and $a_o b_o$ is the cross-sectional area of the chain. For α-phase PP, the crystal growth is estimated in favor along (110) lattice plane during melt-crystallization; for β-phase PP, the crystal growth is estimated in favor along (300) lattice plane. Thus, the value of $a_o b_o$ is 3.44×10^{-19} and 3.50×10^{-19} m^2 for α-PP and β-PP, respectively. And Δh_f is 1.96×10^8 J/m^3 for α-PP and 1.77×10^8 J/m^3 for β-PP [24, 25].

The fold surface free energy σ_e of virgin PP-MA and PP-MA/NA are shown in Table 1 too. As expected, the addition of NA results in smaller K_g and σ_e values. Generally, surface nucleation barrier is positive proportion to K_g [23] and the increase of σ_e goes against the folding of the molecule chain [26]. Beck's theory thought that a good NA reduced the interfacial surface free energy [27]. The

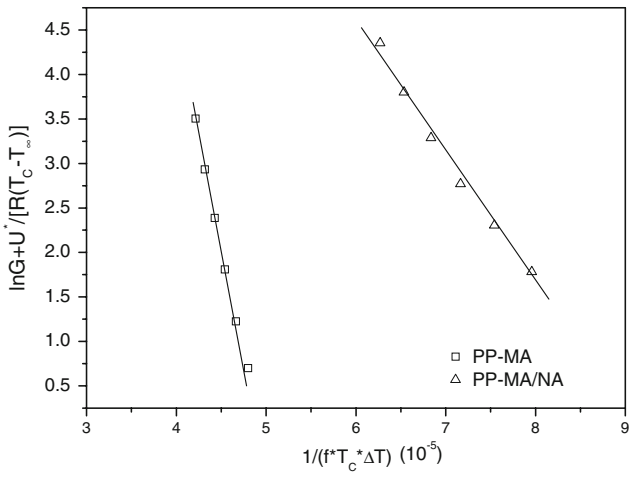

Fig. 6 Plot of $\ln G + U^* /R(T_c - T_\infty)$ vs. $1/T_c \cdot \Delta T \cdot f$ for PP-MA and PP-MA/NA

smaller the σ_e value, the better the nucleation effect of NA is. Table 1 shows that TMB-5 has good nucleation effect for PP-MA.

The lamella thickness formed during the isothermal crystallization process was calculated according to the equation developed by Thomson and Gibbs [28]:

$$T_m = T_m^o[1 - 2\sigma_e/(l\Delta h_f)] \quad (9)$$

where l is the lamellar thickness, T_m, σ_e, and Δh_f are defined as previous. According to Thomson-Gibbs equation, the lamellar thickness of a polymer can be calculated as follows:

$$l = 2\sigma_e T_m^o/[\Delta h_f (T_m^o - T_m)] \quad (10)$$

Prior to calculating the lamellar thickness, one must know the value of equilibrium melting temperature, which can be obtained by linear extrapolating the experimental data to $T_m = T_c$ line based on Hoffman-Weeks theory [26]. Here, the T_m^o for neat PP-MA and PP-MA/NA are calculated as 188.6 and 173.4 °C. As shown in Table 1, the lamella thickness increases with increasing of T_c, indicating more perfect spherulites formation at higher temperature. Furthermore, the addition of NA results in the decrease of lamella thickness, although the nucleated sample crystallizes at relative higher temperature. Considering the main crystal forms in virgin PP-MA (α-phase) and in PP-MA/NA (β-phase), it can be proved that, for PP-MA, α-phase shows bigger lamella thickness than that of β-phase.

Nonisothermal crystallization and subsequent melting behaviors

Study on the nonisothermal crystallization behavior is very important because polymer usually faces the temperature gradients and the crystallization is normally the nonisothermal crystallization during the processing. In this section, the nonisothermal crystallization and subsequent melting behaviors of neat PP-MA and PP-MA/NA were comparatively researched. Figure 7 shows the DSC heating curves of such samples after nonisothermal crystallization at different cooling rates as indicated. Interestingly, neat PP-MA presents double melting peaks, one is present at about 156–159 °C (α_1) and the other (α_2) at 164 °C. α_1 shifts to lower temperatures and gets weaker intensity with the increasing of cooling rate, whereas α_2 keeps invariant temperature but gets stronger intensity. Obviously, the grafted maleic anhydride prevents the nucleation and lamella growth of PP-MA, resulting in the formation of

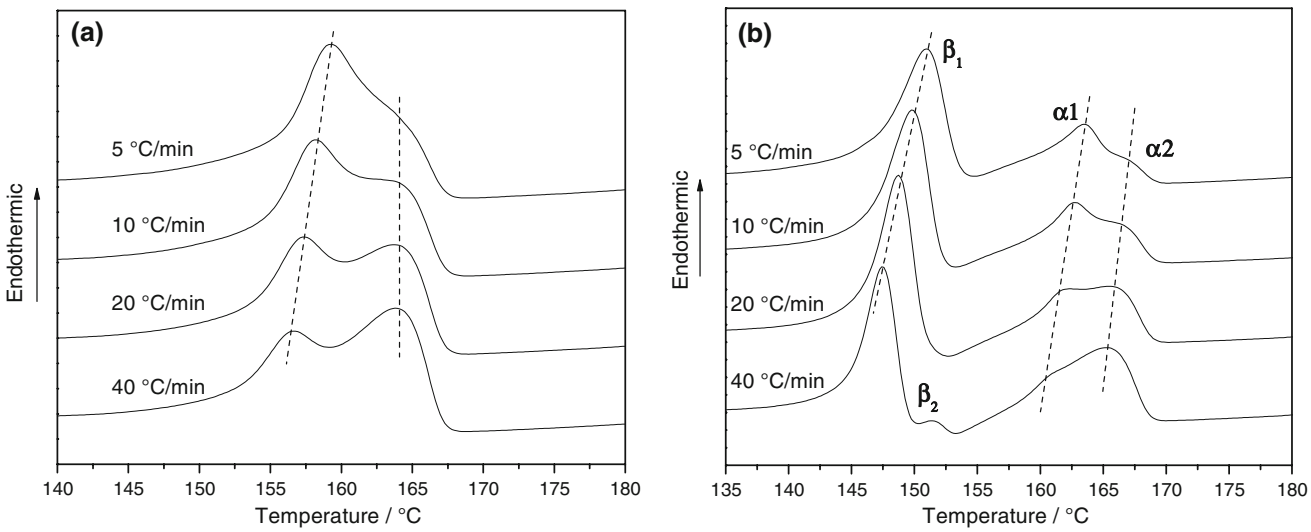

Fig. 7 DSC heating curves of **a** PP-MA and **b** PP-MA/NA after nonisothermal crystallization at different cooling rates. The data show the corresponding cooling rates

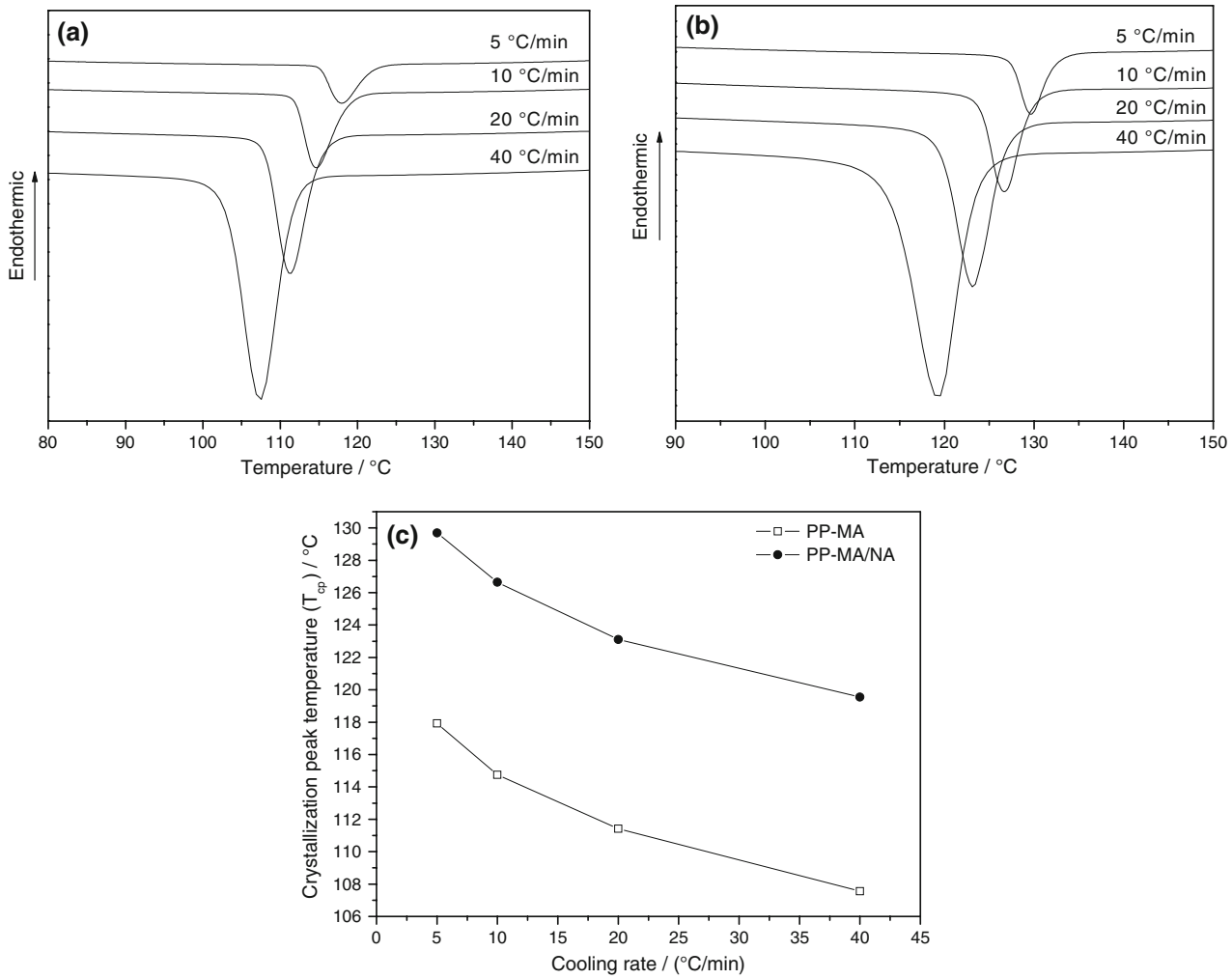

Fig. 8 DSC cooling curves of **a** PP-MA and **b** PP-MA/NA samples during the nonisothermal melt crystallization at different cooling rates. **c** shows the crystallization peak temperature versus cooling rate

spherulites with more defects compared with isotactic PP. Thus, it can be deduced that α_1 is related to the fusion of the lamella with defects and α_2 is attributed to the fusion of lamella formed due to recrystallization or reorganization of lamella initially formed during nonisothermal crystallization [29]. Three melting peaks, 147–151 °C (β), 161–163.5 °C (α_1) and 165–167 °C (α_2), are observed for all the nonisothermal crystallized PP-MA/NA samples. These melting peaks shift to lower temperatures with the increasing of cooling rate, indicating the formation of more imperfect lamella structure. Compared with the melting behavior of isothermal crystallized sample, one can see that nonisothermal crystallized sample exhibits relative lower melting temperature, indicating the formation of lamella with more defects or smaller thickness.

The typical DSC cooling traces obtained at different cooling rates are shown in Fig. 8. Especially, the corresponding crystallization peak temperatures (T_{cp}) at different cooling rates were determined from the cooling curves and the results are shown in Fig. 8 too. For all the samples, the T_{cp} decreases with increasing cooling rate. This is attributed to the dependence of nucleation and crystal growth on the degree of supercooling. A small cooling rate provides better fluidity and diffusivity for molecules due to low viscosity and more time for crystallization, thus inducing higher crystallinity at higher temperature, than for a sample cooled with a fast cooling rate [30]. Neat PP-MA has smaller T_{cp} due to the relative homogeneous nucleation process and the relative low nucleation density. For PP-MA/NA, the T_{cp} is much higher than that of neat PP-MA, further indicating the great nucleation effect of TMB-5 for PP-MA crystallization.

Conclusions

In summary, an aryl amide derivative (TMB-5) has been introduced into PP-MA and the crystallization and subsequent melting behaviors of TMB-5 nucleated PP-MA

have been intensively researched based on isothermal and nonisothermal crystallization process, respectively. The results show that TMB-5 is an efficient β-NA in inducing PP-MA crystallization as β-phase with largely increased crystallization rate, decreased fold surface free energy and decreased lamella thickness.

Acknowledgements Authors would like to express their sincere thanks to National Natural Science and Technology Foundation (No. 50403019), Program for New Century Excellent Talents in University (NCET-08-0823) and Sichuan Youthful Science and Technology Foundation (07ZQ026-003) (P.R. China) for supporting this work.

References

1. Martin O, Roman C, Karel S. Tailoring of three-phase crystalline systems in isotactic poly(propylene). Macromol Rapid Commun. 2005;26:1253–7.
2. Stocker W, Schumacher M, Graff S. Epitaxial crystallization and AFM investigation of a frustrated polymer structure: isotactic poly(propylene), β phase. Macromolecules. 1998;31:807–14.
3. Huo H, Jiang SC, An LJ. Influence of shear on crystallization-behavior of β-phase in polypropylene with β-nucleating agent. Macromolecules. 2004;37:2478–83.
4. Fujiwara Y. Double-melting behavior of the β-phase of isotactic polypropylene. Colloid Polym Sci. 1975;253:273–82.
5. Lovinger AJ, Chua JO, Gryte CC. Studies on the α and β forms of isotactic polypropylene by crystallization in a temperature gradient. J Polym Sci Polym Phys Ed. 1977;15:641–56.
6. Yoshida H. Dynamic analysis of the melting behavior of polymers showing polymorphism observed by simultaneous DSC/X-ray diffraction measurements. Thermochim Acta. 1995;267:239–48.
7. Leugering HJ, Kirsch G. Effect of crystallization from oriented melts on crystal structure of isotactic polypropylene. Angew Makromol Chem. 1973;33:17–23.
8. Varga J, Karger-Kocsis J. Interfacial morphologies in carbon fibre-reinforced polypropylene microcomposites. Polymer. 1995;36:4877–81.
9. Varga J, Ehrenstein GW. Formation of β-modification of isotactic polypropylene in its late stage of crystallization. Polymer. 1996;37:5959–63.
10. Varga J, Karger-Kocsis J. Rules of supermolecular structure formation in sheared isotactic polypropylene melts. J Polym Sci B. 1996;34:657–72.
11. Zhang J, Shen KZ, Na S. Vibration-induced change of crystal structure in isotactic polypropylene and its improved mechanical properties. J Polym Sci B. 2004;42:2385–90.
12. Mathieu C, Thierry A, Wittmann JC, Lotz B. "Multiple" nucleation of the (010) contact face of isotactic polypropylene, α phase. Polymer. 2000;41:7241–53.
13. Romanini D, Guidetti GP. Proceedings of polymer chemistry in extruder, Lie'ge, Belgium: Societe Royale de Chimie, 1990.
14. Bai HW, Wang Y, Liu L, Zhang JH, Han L. Nonisothermal crystallization behaviors of polypropylene with α/β nucleating agents. J Polym Sci B. 2008;46:1853–67.
15. Menyhárd A, Faludi G, Varga J. β-Crystallisation tendency and structure of polypropylene grafted by maleic anhydride and its blends with isotactic polypropylene. J Therm Anal Calorim. 2008;93:937–45.
16. Turner-Jones A, Aizlewood JM, Beckett DR. Crystalline forms of isotactic polypropylene. Makromol Chem. 1964;75:134–54.
17. Romankiewicz A, Tomasz S, Brostow W. Structural characterization of α- and β-nucleated isotactic polypropylene. Polym Int. 2004;53:2086–91.
18. Varga J. β-modification of polypropylene and its two-component sysytems. J Therm Anal Calorim. 1989;35:1891–912.
19. Marco C, Ellis G, Gómez MA, Arribas JM. Isothermal crystallization behavior and melting characteristics of injection sample of nucleated polypropylene. J Appl Polym Sci. 2003;88:2261–74.
20. Avrami M. Kinetics of phase change. III. Granulation, phase change and microstructure. J Chem Phys. 1941;9:177–84.
21. Avalos F, Lopez-Manchado MA, Arroyo M. Crystallization kinetics of polypropylene III. Ternary composites based on polypropylene/low density polyethylene blend matrices and short glass fibres. Polymer. 1998;39:6173–8.
22. Lauritzen JI, Hoffman JD. Extension of theory of growth of chain-folded polymer crystals to large undercoolings. J Appl Phys. 1973;44:4340–52.
23. Hoffman JD, Davis GT, Lauritzen JI. The rate of crystallization of linear polymers with chain folding, chap. 7. In: Treatise on solid state chemistry, vol. III. New York: Plenum Press; 1976.
24. Karger-Kocsis J. Crystallization, melting and supermolecular structure of isotactic polypropylene, chap.3 and Nucleating of polypropylene, chap. 4. In: Poly(propylene) structure, blends and composites, vol. 1. 1st ed. London: Chapman and Hall; 1995.
25. Karger-Kocsis J, Varga J, Ehrenstein GW. Comparison of the fracture and failure behavior of injection-molded α- and β-polypropylene in high-speed three-point bending tests. J Appl Polym Sci. 1997;64:2057–66.
26. Hoffman JD. Regime III crystallization in melt-crystallized polymers: the variable cluster model of chain folding. Polymer. 1983;24:3–26.
27. Beck HN. Heterogeneous nucleating agents for crystallization of vinylidence chloride-vinyl chloride copolymers. J Appl Polym Sci. 1975;19:371–6.
28. Bershtein VA, Egorov VM. Differential scanning calorimetry of polymers: physics, chemistry, analysis. London: Ellis Horwood; 1994.
29. Cho K, Li FK, Choi J. Crystallization and melting behavior of polypropylene and maleated polypropylene blends. Polymer. 1999;40:1719–29.
30. Seo Y, Kim J, Kim KU, Kim YC. Study of the crystallization behaviors of polypropylene and maleic anhydride grafted polypropylene. Polymer. 2000;41:2639–46.